Contribution from the Research School of Chemistry, The Australian National University, GPO Box 4, Canberra, ACT 2601, Australia

Pathological Luminescence Characteristics of *cis*-$[Ir(bpy)_2Cl_2]^+$

Lynne Wallace, Graham A. Heath,* Elmars Krausz,* and Grainne Moran†

Received June 5, 1990

Introduction

Luminescence usually arises from the thermally accessible, lowest excited levels of a system. Fast radiationless and intersystem crossing processes establish an effective thermal equilibrium within the manifold of excited states. Of continuing interest appears to be the occurrence of inorganic complexes having two or more electronic excited states separated by energies comparable to vibrational or lattice phonon energies (1–3000 cm^{-1}), but *without these states being in thermal equilibrium* on the approximate microsecond time scale (dual emitters).

Since the first reports[1-3] of the luminescence of *cis*-$[Ir(bpy)_2Cl_2]^+$ and its analogues, there have been numerous reports of unusual temperature and solvent dependence and particularly of nonexponential decay kinetics with concomitant time dependence of luminescence spectra.[1-12]

Of considerable interest has been the persistent observation of a weak, broad (red) luminescence centered around 680 nm. In fluid DMF solutions at moderately low temperatures, this feature becomes more apparent. It can also dominate the time-resolved spectra taken in frozen DMF, after sufficient delay.[9] The red luminescence becomes significantly stronger when the bpy ligand is perdeuterated, and great pains have been taken to establish it as genuine. A distinctive risetime seen in the red luminescence (for the related phenanthroline complex) helps significantly in this respect.[8]

The view that has evolved from previous work, summarized in Figure 1 (scheme a), is that the luminescence seen in the 460–550-nm (green) region is triplet MLCT luminescence and that the red luminescence arises from the lowest energy, spin-forbidden, metal-centered d–d state. From the temperature dependence of the relative intensity of the red and green emissions, it has been inferred that the d–d state lies ≈370 cm^{-1} below the lowest MLCT state. Deuteration of the bpy ligand was found to apparently increase the gap to 540 cm^{-1}. The MLCT transition shifts relative to the d–d band, favoring the red luminescence.

This basic scenario has been supported by pressure dependence[12] and triplet–triplet absorption[10] studies. The most recent investigation on low-temperature lifetime behavior failed to see evidence, in DMF/water mixtures, for the red emission,[13] but these workers suggested that there may be two distinct types of green emitter.

The apparent lack of thermal equilibrium[8,9] between emitting states at 77 K on the microsecond time scale is unusual. MLCT states quickly undergo strong dielectric relaxation (≈2000 cm^{-1}) in fluid solutions,[16] and in our view the d–d states would not shift to the same extent. Thermal equilibrium is reported in *fluid* solutions, and red luminescence becomes more dominant at lower temperatures. The d–d state thus seems unlikely to lie close below the (unrelaxed, emitting) MLCT in the rigid phase.

This system and its direct analogues are perhaps the best established inorganic dual emitters.[14] Given the continuing interest in this phenomenon, we have incisively reinvestigated this spectroscopically pathological system by using the full range of spectroscopic techniques available in our laboratory.

Experimental Section

$Ir(bpy)_2Cl_2 \cdot Cl$ was prepared from Na_2IrCl_6 by following the method of Watts et al.[15] $Ir(bpy\text{-}d_8)_2Cl_2 \cdot Cl$ was prepared similarly and on the same preparative scale by using perdeutero 2,2′-bipyridine and purified in the same manner. Na_2IrCl_6 was obtained by neutralization of H_2IrCl_6 (Degussa AG) with aqueous NaOH and used without further purification. The trifluoromethanesulfonate (triflate) salt was prepared by metathesis.

Most spectra were collected on a single flexible apparatus, centered around an Oxford Instruments SM4 cryomagnet, a Spex 1704 monochromator, and a Tektronix 2430 digital scope. Details are provided in a number of recent papers[16-31] that concentrate on related ruthenium

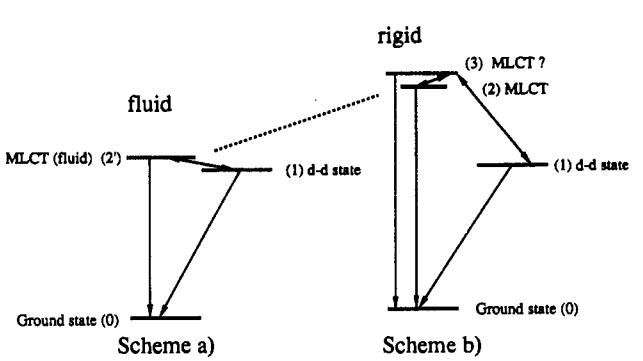

Figure 1. Scheme a: fluid solution model of Watts et al.[9] where the d–d state (1) lies 370 cm^{-1} below the ^{3}MLCT state (2′). k_{20} and k_{10} connect the MLCT and the d–d state with the ground state. Connecting these excited states are k_{12} and k_{21} and for thermal equilibrium k_{12}, $k_{21} >> k_{10}$, k_{20}. Scheme b: MLCT state (2) shifted 2–3000 cm^{-1} above (1) in the rigid phase. (2) does *not* link with (1) ($k_{21} = 0$) but couples via a higher state (3) at elevated temperatures, k_{10} and perhaps k_{30} are dominantly nonradiative.

(1) DeArmond, M. K.; Hillis, J. E. *J. Chem. Phys.* **1971**, *54*, 2247.
(2) Watts, R. J.; Crosby, G. A. *J. Am. Chem. Soc.* **1971**, *93*, 3184.
(3) Watts, R. J.; Crosby, G. A.; Sansregret, J. L. *Inorg. Chem.* **1972**, *11*, 1474.
(4) Watts, R. J.; White, T. P.; Griffith, B. G. *J. Am. Chem. Soc.* **1975**, *97*, 6914.
(5) Ballardini, R.; Varani, G.; Moggi, L.; Balzani, V.; Olson, K. R.; Scandola, F.; Hoffman, M. Z. *J. Am. Chem. Soc.* **1975**, *97*, 728.
(6) Watts, R. J.; Griffith, B. G.; Harrington, J. S. *J. Am. Chem. Soc.* **1976**, *98*, 674.
(7) Ballardini, R.; Varani, G.; Moggi, L.; Balzani, V. *J. Am. Chem. Soc.* **1977**, *99*, 6881.
(8) Watts, R. J.; Missimer, D. *J. Am. Chem. Soc.* **1978**, *100*, 5350.
(9) Watts, R. J.; Efrima, S.; Metiu, H. *J. Am. Chem. Soc.* **1979**, *101*, 2742.
(10) Ohashi, Y.; Kobayashi, T. *Bull. Chem. Soc. Jpn.* **1979**, *52*, 2214.
(11) (a) Divisia, B.; Ford, P. C.; Watts, R. J. *J. Am. Chem. Soc.* **1980**, *102*, 7264. (b) Watts, R. J. *Inorg. Chem.* **1980**, *20*, 2302.
(12) DiBenedetto, J.; Watts, R. J.; Ford, P. C. *Inorg. Chem.* **1984**, *23*, 3039.
(13) Ohashi, Y.; Nakamura, J. *Chem. Phys. Lett.* **1984**, *109*, 301.
(14) DeArmond, M. K.; Carlin, C. M. *Coord. Chem. Rev.* **1981**, *36*, 325.
(15) Watts, R. J.; Harrington, J. S.; Van Houten, J. *J. Am. Chem. Soc.* **1977**, *99*, 2179.
(16) Ferguson, J.; Krausz, E. *Inorg. Chem.* **1986**, *25*, 3333.
(17) Ferguson, J.; Krausz, E. *Chem. Phys. Lett.* **1986**, *127*, 551.
(18) Ferguson, J.; Krausz, E. *J. Lumin.* **1986**, *36*, 129.
(19) Ferguson, J.; Krausz, E. *J. Phys. Chem.* **1987**, *91*, 3161.
(20) Ferguson, J.; Krausz, E. *Chem. Phys.* **1987**, *112*, 271.
(21) Krausz, E. *Chem. Phys. Lett.* **1987**, *135*, 249.
(22) Krausz, E. *J. Chem. Soc., Faraday Trans.* **1988**, 84, 827.
(23) Krausz, E.; Moran, G. *J. Lumin.* **1988**, *40*, *41*, 272.
(24) Krausz, E. *J. Lumin.* **1988**, *42*, 283.
(25) Krausz, E. *Inorg. Chem.* **1988**, *27*, 92.
(26) Krausz, E.; Moran, G. *J. Lumin.* **1988**, *41*, 20.
(27) Riesen, H.; Krausz, E.; Puza, M. *Chem. Phys. Lett.* **1988**, *151*, 65.
(28) Riesen, H.; Krausz, E. *Chem. Phys. Lett.* **1988**, *151*, 71.
(29) Krausz, E.; Moran, G. *J. Chem. Phys.* **1989**, *90*, 39.
(30) Krausz, E.; Moran, G.; Riesen, H. *Chem. Phys. Lett.* **1990**, *165*, 401.
(31) Krausz, E. *Chem. Phys. Lett.* **1990**, *165*, 407.

† Present address: Department of Analytical Chemistry, University of New South Wales, Kensington, NSW 2033, Australia.

0020-1669/91/1330-0347$02.50/0 © 1991 American Chemical Society

bipyridyl type systems. That experience has been indispensable in developing adequate instrumentation and techniques in order to study this difficult system.

Results

Decay Characteristics. Luminescence decay kinetics were accumulated for the protonated and deuterated complexes, as the neat chloride powders, in frozen DMF and in EM (4:1 ethanol/methanol) glasses. Measurements were also made on single crystals of the triflate salt.

Kinetics were accumulated by using both long (millisecond) pulse, Bragg cell modulated Ar^+ ion excitation at 458, 488, and 514 nm and short (3-5 ns) N_2 dye/laser pulses at 337 and 440 nm. Decay kinetics were found to be strongly dependent on temperature in the range 1.6–77 K as well as on the excitation energy and detected wavelength of the luminescence.

Decay kinetics were measurably nonexponential above 20 K. Attempts were made to analyze entire *families* of decay curves, measured across the luminescence spectrum, using the global procedure of Krausz.[24]

A global single-exponential fit of 36 decay profiles, with 3-ns excitation at 337 nm, measured at equally spaced energies spanning the entire emission, of the protonated and deuterated species in DMF at 77 K, provided best fit lifetimes of 3.8 and 3.85 μs, respectively. The fits were poor and residuals systematic, and this situation was not usefully improved by a global dual-exponential fit. The best fit dual "lifetimes" were 1.6 and 4.7 μs for the protonated complex and 2.0 and 5.8 μs for the deuterated complex. The largest residual intensities were always associated with the green, rather than the red, emission.

Similar behavior was observed in EM. This environment, the defacto standard in the field, forms a clear glass, whereas DMF forms a strongly scattering, polycrystalline matrix at 77 K. $[Ru(bpy)_3]^{2+}$ decay kinetics were measured in frozen DMF in order to prove the effect of the polycrystalline environment. Good global single-exponential behavior was obtained with a uniform lifetime of 5.1 μs, entirely in accord with work done on this well-established system in a number of environments.[24]

At 77 K, the decay curves obtained by exciting at 488 and 515 nm approached exponential behavior and lifetimes were uniformly longer; in DMF the protonated lifetime fits gave 12–13 μs and the deuterated, 15–19 μs, exciting at 488 nm, detecting from 547 to 703 nm.

At 4.2 K, with excitation at 458 nm, decays became *quantitatively* exponential across the luminescence. The protonated (h_8) and deuterated (d_8) samples in DMF gave 92 ± 1 and 107 ± 1 μs, respectively. Excitation at either 488 or 514 nm gave *shorter* (but not single exponential) lifetimes of around 20 and 40 μs, respectively.

Short-pulse excitation at 337 nm at 4.2 K, did not give accurately exponential decays, even at the lowest excitation fluences. Dye laser excitation at 440 nm gave decay times almost identical with the long-pulse 458-nm excitation values. The 337-nm excited decays showed greatest deviation from single-exponential behavior in the red region, where a second component of 20 or 40 μs became evident, for the h_8 or d_8 material, respectively.

Decay kinetics, detected at 547 nm, with long-pulse excitation at 458 nm, were measured as a function of temperature between 1.7 and 80 K, for the protonated and deuterated species, in both DMF and EM. As well as the decays becoming obviously nonexponential above 20 K, it was significant that under constant (long pulse) excitation conditions, the initial amplitude of the decay profile remained virtually constant. Similar behavior was seen for all systems.

Decay profiles of the neat chloride salts were more complex than those in dilute media. At 77 K, very little green emission is seen, and only a little at 4 K. For the red emission decay times are comparable to those in dilute media, but there is clear evidence for energy transfer and impurity trapping.

Luminescence and MCPL. The 458-nm Ar^+ laser line is virtually coincident with the origin feature of the MLCT absorption. Figures 2 and 3 show time-resolved spectra, excited at 337 nm. At longer times in the 77 K spectra (Figure 2), but at (relatively)

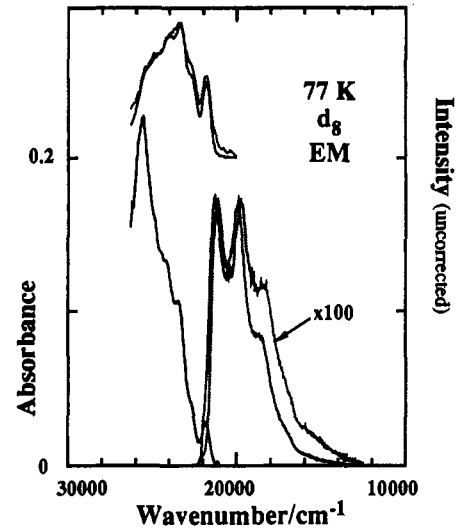

Figure 2. Lower left: absorption spectrum of $Ir(bpy\text{-}d_8)_2Cl_2^+$ in EM at 77 K. Directly above are excitation spectra detected at 547 nm (—) and 640 nm (···). Time-resolved luminescence spectra taken after 1 μs (—) and 30 μsec (···) are on the right.

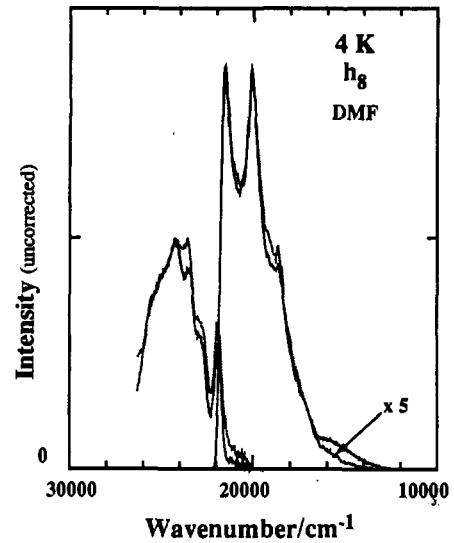

Figure 3. Excitation spectra of $Ir(bpy\text{-}d_8)_2Cl_2^+$ in DMF at 4.2 K detected at 547 nm (—) and 640 nm (···). Time-resolved luminescence spectra taken after 10 μs (—) and 100 μs (···) are on the right.

shorter times in the 4.2 K spectra (Figure 3), the red band is clearly revealed. It is invariably a minor component of the total luminescence in the rigid phase.

Steady-state spectra, excited at 488 or 515 nm, however, show the red emission very strongly enhanced. Also present, to a variable extent, is a yellow emission at around 560 nm. This (yellow) emission dominates the luminescence of chloride powders with any excitation energy, but is much weaker in our best single crystals of the triflate salt. It appears to be associated with the strongly emitting impurity of the type previously reported.[5,7]

MCPL spectra were measured by using 458-, 488-, and 515-nm excitation (in isotropic EM glasses) in the 1.6–50 K range. With 458-nm excitation, a negative B term type signal ($\Delta I/I \approx 0.05$ at 3 T) was obtained between 1.6 and 10 K, which diminished at higher temperatures. With 488-nm excitation, the MCPL magnitude was greatly reduced ($\Delta I/I < 0.01$) in the red region. This indicates that the 488-nm excited luminescence has an entirely different character, with weak MCPL.

Excitation, Absorption, and MCD. Absorption and excitation spectra are shown in Figures 2–4. From a comparison of absorption and excitation spectra of powders, crystals, and glasses, we are able to determine the shift of the lowest origin feature upon deuteration of the bpy as 30 ± 10 cm^{-1}. This compares rather

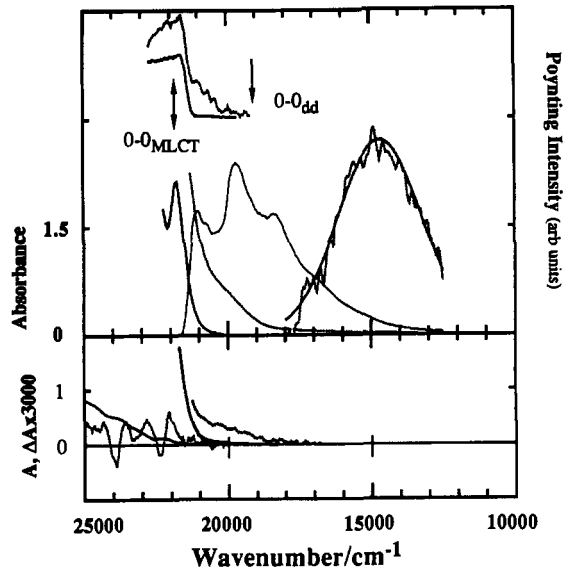

Figure 4. Lower panel: absorption (—) MCD (···) at 5 T and 4.2 K of Nafion films[22] with differing concentrations of $Ir(bpy)_2Cl_2^+$. Lower left of the upper panel shows the 300 K absorption spectrum of a ≈10 μm thick (chloride) crystal (—) and ≈300 μm thick triflate crystal. Directly above are 4.2 K (uncorrected) excitation spectra of the (triflate) crystal detected at 547 nm (—) and 640 nm (···). Also shown is the 5 K luminescence spectrum, excited at 458 nm, of the pure triflate crystal. The right-hand side shows the "pure" d-d luminescence, calculated by subtracting 10- and 200-μs time-resolved spectra in DMF at 4 K with the least-squares fit Gaussian curve.

well with the value of 40 cm^{-1} seen in analogous MLCT transitions in $[Ru(bpy)_3]^{2+}$.[27,28,30]

Excitation spectra are dependent upon the energy of detection. With red (640 nm) detection, a broad feature is seen in the 490–520-nm region that is absent when green (547 nm) detection is used. This low-energy feature is seen most clearly in the excitation spectrum of the single-crystal triflate salt (Figure 4). An absorption feature in this region can also be seen with a moderately thick crystal.

The MCD spectra (Figure 4), taken in dilute and very concentrated Nafion films, show a low-energy feature with electronic properties clearly different from that of the lowest MLCT transitions.

Discussion

Our results clearly identify a weak transition below the MLCT state. Subtraction of appropriately scaled, time-resolved luminescence spectra allow us to extract the "pure" red emission (Figure 4). This spectrum is well fitted by a Gaussian curve, centered at 14 700 cm^{-1} (680 nm) with a width of 3400 cm^{-1}. Comparing this to absorption and excitation spectra it seems reasonable to estimate the origin of the band to be around 19 000 cm^{-1} (530 nm), ≈3000 cm^{-1} below the MLCT origin.

A three-level system such as scheme a (Figure 1) will, in general, give only dual-exponential behavior[32] irrespective of the values of k_{10}, k_{20}, k_{21}, and k_{12}. Our data do not fit such a model at all, and it becomes necessary to introduce an additional excited state (scheme b).

The presence of an additional level, which is strongly coupled (nonradiatively) to the ground state via the low-efficiency red emitting state is entirely consistent with our data. In particular, the reduction in lifetimes, *but with constant initial intensity*, observed in the 20–80 K range reflects a fall in quantum efficiency and not the population of a more strongly radiative electronic state. The presence of close-lying MLCT states with different electronic properties is well established in this type of complex.[33]

The magnitude of the deuteration shift of the MLCT band determined in this work is inconsistent with the previous analysis.[9] That the d–d and MLCT processes have different relaxation shifts (Figure 2), pointed out for the first time in this work, was not taken into account. An adequate analysis of the relative intensities of the red and green emissions in viscous solutions clearly requires more detailed consideration of the extent of thermal equilibrium and the dielectric relaxation process.

Acknowledgment. We thank Miroslav Puza for the perdeuterated 2,2′-bipyridine and Lucjan Dubicki, Mark Riley, and Hans Riesen for invaluable discussions and input. L.W. thanks Celltech U.K. for financial support.

(32) Matsen, F. A.; Franklin, J. L. *J. Am. Chem. Soc.* **1950**, *72*, 3337.
(33) Krausz, E.; Ferguson, J. *Prog. Inorg. Chem.* **1989**, *37*, 293.

Contribution from the Department of Chemistry and Laboratory for Molecular Structure and Bonding, Texas A&M University, College Station, Texas 77843

A New Look at the Vanadium(III) and Vanadium(IV) Complexes of the Dibenzotetramethyltetraaza[14]annulene Ligand. Synthesis and Molecular Structures of CpV(tmtaa) and (O)V(tmtaa)

F. A. Cotton,* J. Czuchajowska, and X. Feng

Received May 1, 1990

We are currently exploring the chemistry of the title macrocyclic ligand (see **1**), which can form both mononuclear and binuclear complexes. In the binuclear ones, the potential steric repulsion

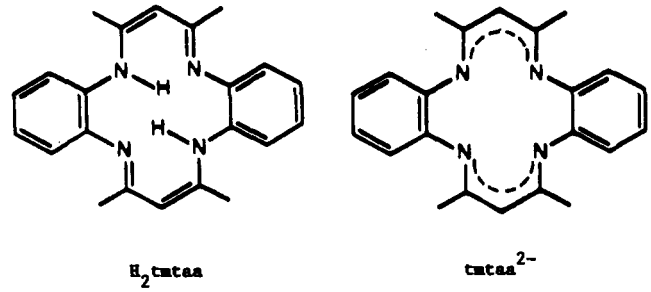

1

of this macrocyclic ligand surprisingly does not seem to affect their stability. In our studies, we have succeeded in synthesizing many interesting mononuclear complexes such as Cr(tmtaa)Cl[1] and $Ru(tmtaa)(PPh_2Me)_2$,[2] among others, and a few fascinating unbridged metal–metal-bonded dimers of the type $M_2(tmtaa)_2$ where M = Cr,[3] Mo,[3] and Rh.[4] The ability of tmtaa to stabilize these and other compounds can be attributed to its two important features: (1) the ability to displace the metal out of the N_4 plane and (2) its flexibility to adjust the saddle shape conformation according to the size of a metal and the axial ligand.

We have decided to use this macrocyclic ligand in reactions with some vanadium starting materials because of the rather unexplored low-valent chemistry of this early transition metal. We were faced however with a 2-fold challenge, in this area of chemistry: (1) the choice and the availability of the appropriate V(II) starting materials are limited, and (2) there is a strong tendency of the low-valent vanadium materials to abstract oxygen from other molecules in the reaction solution. We report here the experimental and theoretical results on two previously communicated but never crystallographically characterized V(III) and V(IV) compounds, which were obtained by interacting the va-

(1) Cotton, F. A.; Czuchajowska, J.; Falvello, L. R.; Feng, X. *Inorg. Chim. Acta* **1990**, *172*, 135.
(2) Cotton, F. A.; Czuchajowska, J. *Polyhedron* **1990**, *9*, 1221.
(3) Cotton, F. A.; Czuchajowska, J.; Feng, X. *Inorg. Chem.* **1990**, *29*, 4329.
(4) Cotton, F. A.; Czuchajowska, J. Unpublished results.

0020-1669/91/1330-0349$02.50/0 © 1991 American Chemical Society